Ionic structure in the aqueous electrolyte glass $LiCl \cdot 4D_2O$

1997 J. Phys.: Condens. Matter 9 8835

(http://iopscience.iop.org/0953-8984/9/42/002)

J. Phys.: Condens. Matter **9** (1997) 8835–8847. Printed in the UK PII: S0953-8984(97)82643-4

Ionic structure in the aqueous electrolyte glass $LiCl \cdot 4D_2O$

S Ansell†, J Dupuy-Philon‡, J-F Jal‡ and G W Neilson§‖

† Material Science Division, Argonne National Laboratory, 9700 South Cass Avenue, Argonne, IL 60439, USA

‡ Departement de Physique de Materiaux, Universite Claude Bernard, 69622 Villeurbanne Cédex, France

§ H H Wills Physics Laboratory, University of Bristol, Tyndall Avenue, Bristol BS8 1TL, UK

Received 17 March 1997, in final form 14 July 1997

Abstract. The difference methods of neutron diffraction and isotopic substitution were applied to Li^+ and Cl^- in the aqueous lithium chloride glass $LiCl \cdot 4D_2O$ at 120 K (the glass transition $T_g = 150$ K). Results for the ionic hydration show that structural changes are more evident for the Cl^- coordination than for the Li^+ coordination. At the level of the anion–anion structure there is an appreciable increase in the nearest-neighbour coordination number over that in the liquid which suggests a greater degree of correlation between the Cl^- anion and the water molecules. A model of the ionic structure is proposed to explain the relative ease of glassification of concentrated aqueous lithium chloride solutions.

1. Introduction

Lithium chloride–water mixtures are well suited to the study of fragile glass formation [1]; a range of concentrations exists over which glass formation is relatively easy [2]. For two mixtures in particular, $LiCl \cdot 4H_2O$ and $LiCl \cdot 6H_2O$, a variety of methods have been used to characterize the glassification process. The atomic structure of both systems has been recently studied by the method of neutron diffraction and isotopic substitution (NDIS) [3, 4]. The use of H/D substitution shows that the water structure, as defined through the partial pair radial distribution function $g_{HH}(r)$, and linear combinations of the other radial distributions functions, is 'even more severely disrupted' in the tetrahydrate than in the hexahydrate [4].

As a continuation of this work, attention is focused on the structure of the ions in the glassy state, and is aimed at identifying a structural signature associated with glassification such as might be anticipated from the work of Angell and Sare [1]. Recall that in their classic paper on fragile glasses they demonstrated that aqueous electrolyte glasses could be classified according to the anions present in the system. In particular they showed that metal chloride hydrates and metal nitrate hydrates formed two groups of glassy compounds. Because NDIS is particularly well adapted to the study of systems containing chlorine [5], a study was made of Cl^- hydration and the solute structure defined by the pair distribution function $g_{ClCl}(r)$ in $LiCl \cdot 4D_2O$. A complementary study of Li^+ coordination was also made to investigate the extent of changes in Li^+ hydration on glassification. The results were compared with those obtained in previous NDIS experiments on liquid lithium chloride solutions [6–13], and used to provide new insights into the nature of glassification of aqueous electrolytes.

‖ Please send correspondence and reprint requests to G W Neilson, University of Bristol.

0953-8984/97/428835+13$19.50

2. Experimental details

2.1. Sample preparation

Five sample solutions of *Li*Cl (table 1) were prepared directly from a mixture of isotopically labelled solutions of lithium hydroxide, $LiOH_{(aq)}$, and hydrochloric acid, $HCl_{(aq)}$. The isotopically labelled *lithium hydroxide was prepared by the dissolution of *Li metal in water: the *Li was washed in ethyl alcohol to remove the oil in which the metal was stored, dried in air and added in small pieces to chilled distilled water in the manner described by Vogel [14]. The isotopically labelled hydrochloric acid was made by elution of sodium chloride (Na*Cl) solution through an Amberlite 120H ion exchange resin, described in detail by BDH [15]. Excess acid was added to the hydroxide solution and the resultant *Li*Cl solution was filtered through C-18 filters to remove traces of oil and other hydrophobic contaminants. The purified solution was evaporated to dryness under vacuum at a temperature $\sim$300 °C to produce solid *Li$^{*}Cl_{(s)}$. Each *Li$^{*}Cl_{(s)}$ was added to excess D_2O and gently boiled down to near dryness, with heavy water being added about four or five times until the H_2O content (checked by IR spectroscopy) was sufficiently low ($< 0.4\%$) (table 1). Each solution was then boiled down to the correct molality. Samples were then checked for isotopic content by mass spectrometry, light-water impurity (IR spectrometry) and ionic concentration (conductivity and colorimetry) (tables 1 and 2). They were then sealed in glass containers and transported to Saclay.

Table 1. The atomic fractions of the samples *Li*Cl $\cdot$ 4D_2O. The sample number density, ρ, was 0.092 atoms Å^{-3} at 20 °C and was assumed to be unchanged in the glass.

Solute	$c_{^7Li}$	$c_{^6Li}$	$c_{^{35}Cl}$	$c_{^{37}Cl}$	c_D	c_H	c_O
$^7Li^{35}Cl$	0.0688	0.0026	0.0680	0.0035	0.567	0.004	0.285
$^7Li^{NAT}Cl$	0.0714	0.000	0.0541	0.0173	0.567	0.004	0.285
$^7Li^{37}Cl$	0.0713	0.0001	0.0645	0.00689	0.567	0.004	0.285
$^{\phi}Li^{NAT}Cl$	0.0330	0.0384	0.0541	0.0173	0.567	0.004	0.285
$^6Li^{NAT}Cl$	0.007	0.0707	0.0541	0.0173	0.567	0.004	0.285

Table 2. The mean neutron coherent scattering length b (fm) of the constituent atoms in each of the five samples. The deuterium was contaminated with 0.4% H.

	Lithium	Chlorine	Oxygen	Deuterium
$^7_{35}F(Q)$	−2.06	11.49	5.805	6.60
$^7_{NAT}F(Q)$	−2.22	9.579	5.805	6.60
$^7_{37}F(Q)$	−2.22	3.59	5.805	6.60
$^6_{NAT}F(Q)$	1.96	9.579	5.805	6.60
$^{\phi}_{NAT}F(Q)$	0.01	9.579	5.805	6.60

2.2. Instrumental set-up

The experiment was carried out on the 7C2 diffractometer at Saclay with an incident neutron beam of 0.701 Å which was collimated by two cadmium insets of 10 mm width and 50 mm

height. Another cadmium inset was used to shield the detectors from scattering from the aluminium walls of the front of the bell jar. This was the only collimation used during the experiment. (Because there was no secondary collimation on the detectors, the background was large and found to have an appreciable sample dependent component.) The wavelength of the neutrons and orientation of the banana detector were calculated from nickel powder diffraction data.

The samples were maintained in their cold glassy state at 120 K in an 'orange' cryostat. The design of this cryostat allows the sample to be positioned in the beam between two 1 mm thick vanadium foil heat shields at the neutron beam level. The temperature was controlled by dripping liquid helium onto a small heater which was thermally anchored to the inner heat shield and the top of the sample. This arrangement allowed the temperature and the temperature gradient across the sample to be controlled to ± 1 K and ± 0.2 K cm^{-1} respectively.

The liquid samples were glassified as follows. The vanadium container with its liquid sample was attached to the candlestick mounting of the cryostat. The container and end part of the candlestick mounting were then plunged into liquid nitrogen; the rapid cooling ensured no crystallization took place (see figure 1). The candlestick with its sample on the end were quickly transferred to the cryostat and brought to thermal equilibrium at 120 K in about half an hour. Data were collected for all samples at this temperature which is well below the glass transition temperature, $T_g = 150$ K [2].

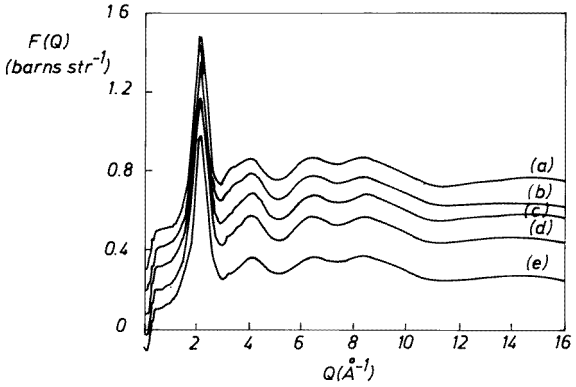

Figure 1. The total structure functions, ${}^{*}_{*}F(Q)$, for the five isotopically labelled $^{*}Li^{*}Cl \cdot 4D_2O$ glasses at 120 K: (*a*) ${}^{6}_{NAT}F(Q) + 0.3$; (*b*) ${}^{\phi}_{NAT}F(Q) + 0.2$; (*c*) ${}^{7}_{35}F(Q) + 0.1$; (*d*) ${}^{7}_{NAT}F(Q)$; (*e*) ${}^{7}_{37}F(Q) - 0.1$.

2.3. Data acquisition and treatment

Neutron diffraction data were collected for five solutions in the glassy state ($^{7}Li^{NAT}Cl$, $^{6}Li^{NAT}Cl$, $^{\phi}Li^{NAT}Cl$, $^{7}Li^{37}Cl$, $^{7}Li^{35}Cl$, each with $4D_2O$ per molecule of salt), the empty cryostat, the empty cell in the cryostat, a cadmium rod in the cryostat and a 0.6 cm diameter vanadium rod which was used for data normalization. The data were treated by standard methods for multiple scattering, normalization and absorption correction [16], and the respective structure factors (${}^{7}_{NAT}F(Q)$, ${}^{6}_{NAT}F(Q)$, ${}^{\phi}_{NAT}F(Q)$, ${}^{7}_{37}F(Q)$ and ${}^{7}_{35}F(Q)$) were calculated (figure 1). Two main problems were encountered in the data reduction—one associated with the background subtraction and the other arising from kinematic or 'Placzek' corrections.

The background subtraction, even when large, is of minor importance in a difference experiment if the total cross-sections are similar in all the samples. This is because the real background is similar for all samples, thus inaccuracies in its determination are removed when taking differences. However, lithium and chlorine isotopes have significantly different absorption cross-sections, resulting in larger beam attenuation in samples containing ^{6}Li and ^{35}Cl, which corresponds to a smaller real background scattering. In order to obtain some indication of the extent of this effect, data were collected for a cadmium rod of exactly the same diameter as the sample. The background was found to be approximately one and a half times bigger for a non-absorbing sample than a completely absorbing sample. A modified correction procedure, which gave self-consistent results, was introduced to remove most of the background from the very highly absorbing samples, the remainder having no significant effect on the structural information extracted from the data. The procedure involved making the cadmium spectrum closer to that for a perfectly absorbing spectrum by the removal of the scattering at high angles. For $2\theta < 90^{\circ}$ the cadmium spectrum was unchanged; however, above this angle it was possible for neutrons to scatter directly from the surface of the cadmium rod into the detectors without being absorbed. The area of unattenuated cadmium scattering seen by the cadmium rod was

$$\text{area} = hr\left(2\theta - \sin^{-1}\left(\frac{r}{D}\right)\right) \approx hr\,2\theta \tag{1}$$

where h is the beam height, r is the radius of the cadmium rod and D is the distance from the sample to the detector. The equivalent scattering from a plate of thickness 0.5 mm and area $hr\,2\theta$ with a cross-section equivalent to the cadmium high-Q limit was subtracted from the measured cadmium spectrum. This procedure enabled the calculation of the 'corrected' cadmium background, which was assumed to be the background due to a total absorbed. A linear combination of the 'corrected' cadmium background and experimentally determined empty cryostat background weighted to the calculated sample transmission was then used to produce the sample backgrounds. These new backgrounds replaced the experimentally measured background in the correction procedures.

The Placzek correction is a major problem for systems which contain water because the Placzek series for the deuterium atom does not converge very rapidly and that for hydrogen does not converge at all. This problem becomes compounded when ^{6}Li and ^{7}Li are present, because of the relatively large mass difference between the two isotopes, and the high absorption of the ^{6}Li. Because of this, it was necessary to apply Placzek corrections. It was understood that these would not correct for the deuterium atoms adequately but this was not significant as all the samples had the same deuterium content. The overall effect of this correction was to give ${}^{6}_{NAT}F(Q)$, ${}^{7}_{NAT}F(Q)$ and ${}^{7}_{35}F(Q)$ the same average slopes for $Q > 10$ Å^{-1} (figure 1).

The final structure factors ${}^{*}_{*}F(Q)$ are related to the partial structure factors $S_{\alpha\beta}$ of the system as follows:

$${}^{*}_{*}F(Q) = \sum_{\alpha}\sum_{\beta} c_{\alpha}c_{\beta}\bar{b}_{\alpha}\,\bar{b}_{\beta}(S_{\alpha\beta}(Q) - 1) \tag{2}$$

where c_{α} is the atomic fraction of species α whose mean coherent neutron scattering length is $\bar{b}_{\alpha}$, and the double sum extends over the four atomic species D, O, Li and Cl.

3. Results

The experimental data enabled the direct determination of $G_{Li}(r)$, $G_{Cl}(r)$, and $g_{ClCl}(r)$ in the aqueous lithium chloride glass ($LiCl \cdot 4D_2O$) at 120 K.

3.1. Lithium hydration

The total scattering cross-sections, ${}^{6}_{NAT}F(Q)$ and ${}^{7}_{NAT}F(Q)$, were used to determine the first-order difference function $\Delta_{Li}(Q)$ given by

$$\Delta_{Li}(Q) = {}^{6}_{NAT}F(Q) - {}^{7}_{NAT}F(Q). \tag{3}$$

The $\Delta_{Li}(Q)$ was corrected for residual self-scattering and Placzek effects by subtraction of a second-order Chebychev polynomial, and can be written explicitly as

$$\begin{aligned}\Delta_{Li}(Q) = {} & A_1[S_{LiO}(Q) - 1] + B_1[S_{LiD}(Q) - 1] + C_1[S_{LiCl}(Q) - 1] \\ & + D_1[S_{LiLi}(Q) - 1]\end{aligned} \tag{4}$$

where

$$\begin{aligned} A_1 &= 2c_{Li}c_O\bar{b}_O(\bar{b}_{^6Li} - \bar{b}_{^7Li}) \qquad B_1 = 2c_{Li}c_D\bar{b}_D(\bar{b}_{^6Li} - \bar{b}_{^7Li}) \\ C_1 &= 2c_{Li}c_{Cl}\bar{b}_{nCl}(\bar{b}_{^6Li} - \bar{b}_{^7Li}) \qquad D_1 = c^2_{Li}((\bar{b}_{^6Li})^2 - (\bar{b}_{^7Li})^2). \end{aligned} \tag{5}$$

A cosine window function was applied between $Q = 12.0$ Å^{-1} and $Q = 16.0$ Å^{-1} to remove termination ripple from the transform. The Fourier transformation of $\Delta_{Li}(Q)$ (see figure 2) gave the Li^+ radial distribution function ($G_{Li}(r)$) (figure 3(*a*)), which can be expressed as

$$\begin{aligned} G_{Li}(r) &= A_1[g_{LiO}(r) - 1] + B_1[g_{LiD}(r) - 1] + C_1[g_{LiCl}(r) - 1] + D_1[g_{LiLi}(r) - 1] \\ &= 9.90g_{LiO}(r) + 22.8g_{LiD}(r) + 4.1g_{LiCl}(r) - 0.6g_{LiLi}(r) - 26.2. \end{aligned} \tag{6}$$

The features in $G_{Li}(r)$ below $r = 1.7$ Å are considered unreal and were set equal to $G_{Li}(0) = [-(A + B + C + D)]$. The back transformation was calculated and is shown with the original $\Delta_{Li}(Q)$ (figure 2). The difference between the direct Fourier transform and the back Fourier transform (figure 3) is a small slowly varying function which allows a high degree of confidence in the calculated $G_{Li}(r)$. The coordination (or hydration) number $\bar{n}^O_{Li}$ associated with the O atoms of the water correlations can be calculated by integration over the peaks due to Li . . . O

$$n^O_{Li} = \frac{4\pi\rho}{A_1}c_O\int_{r_1}^{r_2} r^2(G_{Li}(r) + E)\,\mathrm{d}r \ldots . \tag{7}$$

Similar calculations can be made for $\bar{n}^D_{Li}$.

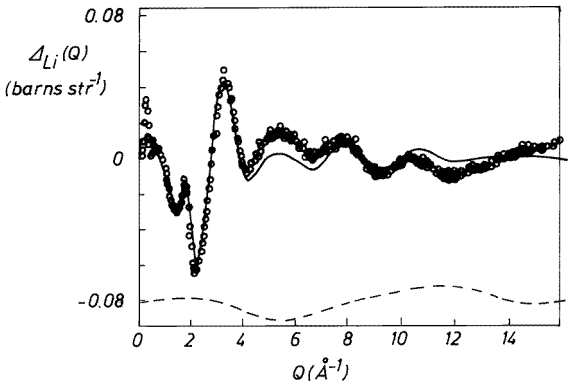

Figure 2. The first-order difference function $\Delta_{Li}(Q)$ for LiCl · 4D$_2$O glass at 120 K. The open circles were calculated from the $F(Q)$ values directly (3), and the full curve is the result of 'back' Fourier transformation of the full curve for $G_{Li}(r)$ (figure 3(*a*)). The slowly varying dashed curve at the bottom is the difference between the two functions shifted by −0.08 barns.

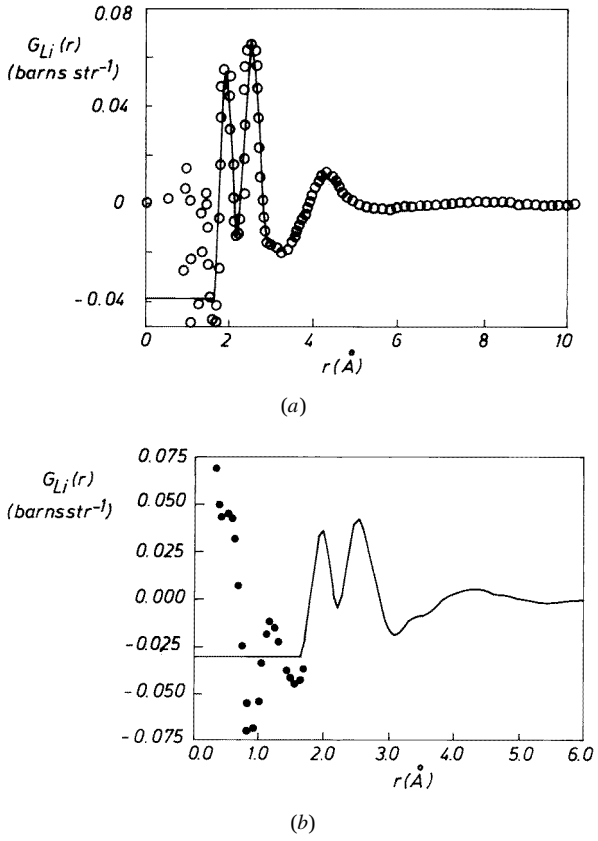

Figure 3. (*a*) The total Li^+ radial distribution function $G_{Li}(r)$ for $LiCl \cdot 4D_2O$ glass at 120 K. The open circles are obtained by direct Fourier transformation of the open-circle curve in figure 2, and the full curve is $G_{Li}(r)$ edited with the data for $r < 1.8$ Å set equal to $G_{Li}(0)$. (*b*) The total Li^+ radial distribution function $G_{Li}(r)$ for $LiCl \cdot 4D_2O$ liquid at 295 K [7, 9].

3.2. Chloride hydration

The total scattering cross-sections ${}^{7}_{35}F(Q)$ and ${}^{7}_{37}F(Q)$ were used to determine the first-order difference function $\Delta_{Cl}(Q)$ given by

$$\Delta_{Cl}(Q) = {}^{7}_{35}F(Q) - {}^{7}_{37}F(Q). \tag{8}$$

The self-scattering term and residual of the Placzek effects were corrected by subtraction of a second-order Chebychev polynomial. The resulting $\Delta_{Cl}(Q)$ (figure 4) can be expressed as

$$\begin{aligned}\Delta_{Cl}(Q) = {} & A_2[S_{ClO}(Q) - 1] + B_2[S_{ClD}(Q) - 1] + C_2[S_{LiCl}(Q) - 1] + D_2[S_{ClCl}(Q) - 1] \\ & + E_2[S_{LiO}(Q) - 1] + F_2[S_{LiD}(Q) - 1] + G_2[S_{LiLi}(Q) - 1]\end{aligned} \tag{9}$$

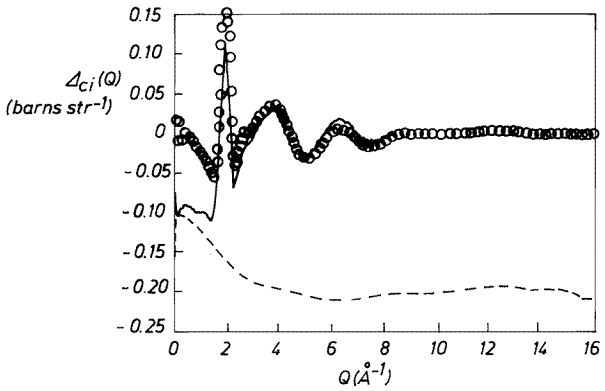

Figure 4. The first-order difference function, $\Delta_{Cl}(Q)$, for LiCl · 4D$_2$O glass at 120 K. The open circles were calculated directly from the $F(Q)$ values (8), and the full curve is the 'back' Fourier transformation of the full curve for $G_{Cl}(r)$ shown in figure 5(*a*). The difference between these two functions is the slowly varying dashed line shifted by −0.2 barns.

where

$$\begin{aligned} A_2 &= 2c_{Cl}c_O\bar{b}_O(\bar{b}_{^{35}Cl} - \bar{b}_{^{37}Cl}) \qquad B_2 = 2c_{Cl}c_D\bar{b}_D(\bar{b}_{^{35}Cl} - \bar{b}_{^{37}Cl}) \\ C_2 &= 2c_{Li}c_{Cl}\bar{b}_{^7Li}(\bar{b}_{^{35}Cl} - \bar{b}_{^{37}Cl}) \qquad D_2 = 2c_{Cl}^2((\bar{b}_{^{35}Cl})^2 - (\bar{b}_{^{37}Cl})^2) \\ E_2 &= 2c_{Li}c_O\bar{b}_O(\bar{b}_{^7Li} - \bar{b}'_{^7Li}) \qquad F_2 = 2c_{Li}c_D\bar{b}_D(\bar{b}_{^7Li} - \bar{b}'_{^7Li}) \\ G_2 &= 2c_{Li}^2((\bar{b}_{^7Li})^2 - (\bar{b}_{^7Li})^2). \end{aligned} \tag{10}$$

$\Delta_{Cl}(Q)$ had a cosine window function applied from 12 Å^{-1} to the end of the data at 16 Å^{-1} and was Fourier transformed to give the chloride radial distribution function $G_{Cl}(r)$ (figure 5(*a*)):

$$\begin{aligned} G_{Cl}(r) &= A_2[g_{ClO}(r) - 1] + B_2[g_{ClD}(r) - 1] + C_2[g_{LiCl}(r) - 1] + D_2[g_{ClCl}(r) - 1] \\ &\quad + E_2[g_{LiO}(r) - 1] + F_2[g_{LiD}(r) - 1] + G_2[g_{LiLi}(r) - 1] \\ &= 17.3g_{ClO}(r) + 39.7g_{ClD}(r) - 1.5g_{LiCl}(r) + 5.7g_{ClCl}(r) - 0.36g_{LiO}(r) \\ &\quad + 0.82g_{LiD}(r) - 0.03g_{LiLi}(r) - 61.63. \end{aligned} \tag{11}$$

The last three terms involving the lithium ion are non-zero because of a small (4%) difference between the lithium isotopic compositions of the $^7Li^{35}Cl$ and $^7Li^{37}Cl$ samples. It is seen from (11) that A_2, $B_2 > C_2$, $D_2 \gg E_2$, F_2, G_2 and consequently the last three terms will not contribute significantly to $G_{Cl}(r)$.

The features in the radial distribution function below $r = 1.95$ Å were deemed to be unphysical and $G_{Cl}(r)$ was set to $G_{Cl}(0)$ for $r < 1.95$ Å and its back transform was determined (figure 4). It shows good agreement with the $\Delta_{Cl}(r)$ calculated directly from the $F(Q)$ values with only low-frequency differences. This suggests that no serious systematic error had arisen in the correction procedures.

The hydration number $n_{Cl}^{D(1)}$ of Cl^- was calculated from

$$n_{Cl}^{D(1)} = 4\pi\frac{\rho}{B_2}c_D\int(G_{Cl}(r) + H)r^2\,\mathrm{d}r\ldots \tag{12}$$

where $H = (A_2 + B_2 + C_2 + D_2 + E_2 + F_2 + G_2) = 61.63$ mb. Evaluation of the integral over the range of the first peak at 2.23 Å gives a value of 4.8 for $n_{Cl}^{D(1)}$.

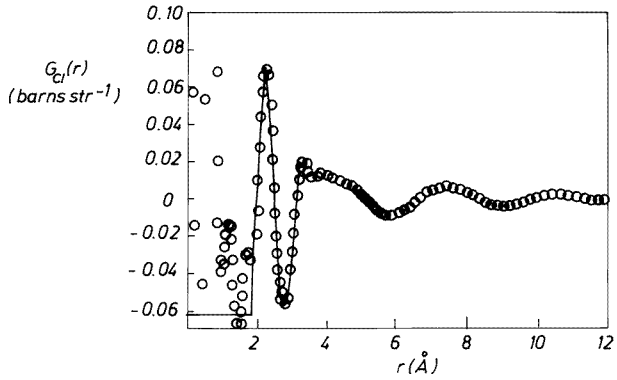

(*a*)

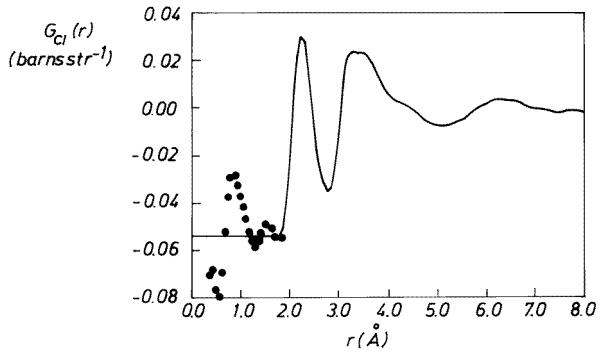

(*b*)

Figure 5. (*a*) The total Cl^- radial distribution function $G_{Cl}(r)$ for $LiCl \cdot 4D_2O$ glass at 120 K. The circles are the Fourier transformation of the open-circle curve for $\Delta_{Cl}(Q)$ in figure 4, and the solid line is $G_{Cl}(r)$ edited with the data for $r < 1.95$ Å set equal to $G_{Cl}(0)$. (*b*) The total Cl^+ radial distribution function $G_{Cl}(r)$ for $LiCl \cdot 4D_2O$ liquid at 295 K [13].

3.3. Anion–anion coordination

The pair correlation function $S_{ClCl}(Q)$ was calculated from a combination of all five factors $F(Q)$:

$$\begin{aligned} S_{ClCl}(Q) &= \alpha\,{}^{7}_{35}F(Q) + \beta\,{}^{7}_{NAT}F(Q) + \gamma\,{}^{7}_{37}F(Q) + \delta\,{}^{\phi}_{NAT}F(Q) + \varepsilon\,{}^{6}_{NAT}F(Q) + \text{corrections} \\ &\equiv 1627\,{}^{7}_{35}F(Q) - 1936\,{}^{7}_{NAT}F(Q) + 476.5\,{}^{7}_{37}F(Q) - 227\,{}^{\phi}_{N}F(Q) \\ &\quad + 60\,{}^{N}_{N}F(Q) + \text{corrections}. \end{aligned} \tag{13}$$

Usually only three, ${}^{7}_{35}F(Q)$, ${}^{7}_{NAT}F(Q)$ and ${}^{7}_{37}F(Q)$, are required [6]. However, because of different amounts of ^{6}Li contamination in the nominally pure ^{7}Li samples of $^7Li^{35}Cl$ and $^7Li^{37}Cl$, we had to include the two additional functions, ${}^{6}_{NAT}F(Q)$ and ${}^{\phi}_{NAT}F(Q)$, to eliminate large contributions from $Li^+ \ldots$ water correlations.

The 'corrections' term in (13) is primarily due to the Cl^- self-scattering, and was determined by an empirical fit of a Chebychev polynomial of order three. In addition, $S_{ClCl}(Q)$ was influenced by two other deficiencies in the data. The first was caused by the

limited accuracy of the values of the scattering lengths b_{Cl} and b_{Li}, which introduced a large uncertainty (∼6%) in the constants in (13). This problem was corrected by allowing the scattering lengths to fluctuate within error, and the use of a fitting routine to find the 'best' values of α, β, δ, γ and ε, that minimized S_{ClCl} for $6 < Q$ (Å^{-1}) < 16. (The assumption that there is little or no significant structural information in $S_{ClCl}(Q)$ for $Q < 6.0$ Å^{-1} has already been demonstrated [6].) $S_{ClCl}(Q)$ determined by this procedure is shown in figure 6.

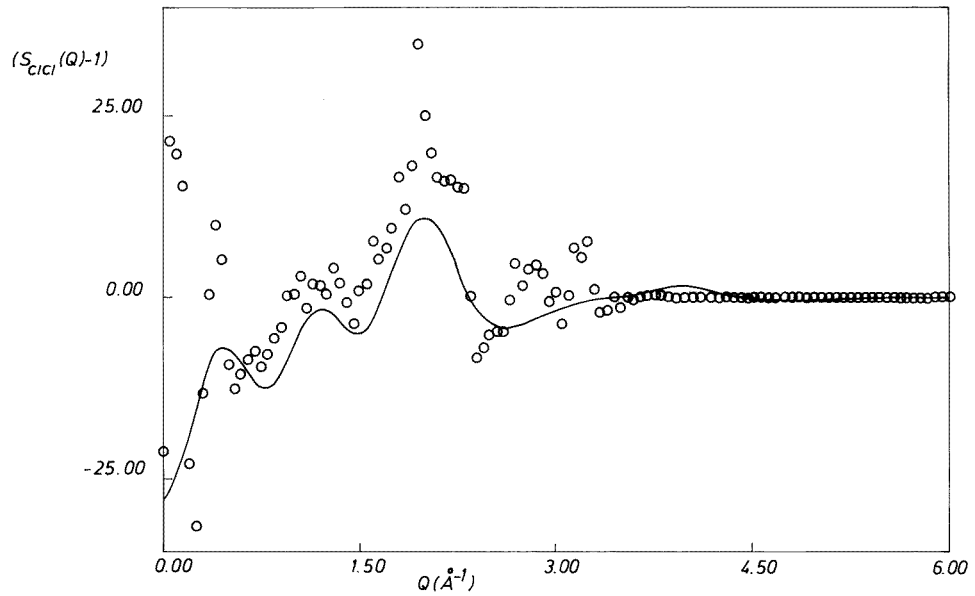

Figure 6. The partial structure factor ($S_{ClCl}(Q) - 1$); the circles were obtained directly from the factors $F(Q)$ (13), and the full curve from self-consistently checks and a maximum-entropy procedure [17] (see the text for details).

The second problem with the data concerned the presence of two sharp peaks, which were clearly visible at 3.3 Å^{-1} and 4.0 Å^{-1} in the original $S_{ClCl}(Q)$. It is justifiably claimed that these peaks arose from ice forming on the aluminium wall of the cryostat's vacuum chamber during the course of the experiment. Consequently their presence in the data could not be properly accounted for in the background subtractions. (It is worth noting that the effect of the ice on the data is sufficiently small that it is not observable in the first-order differences). These Bragg peaks of the ice are of comparable size to the real peaks in $S_{ClCl}(Q)$ and it was assumed that all information in the Q space region of the peaks had been destroyed. As a result, $S_{ClCl}(Q)$, in the region from 3.0 to 4.5 Å^{-1}, was fitted with a cosine window function.

The final $S_{ClCl}(Q)$, together with its maximum-entropy fit, is shown in figure 6 [18]. This fit was necessary due to the noise that resulted from multiplying the factors $F(Q)$ by the five coefficients in (13). The Fourier transform of the maximum-entropy fit is shown in figure 7. The maximum-entropy fit to the data is sufficiently close that a reasonable degree of confidence in the data can be assumed.

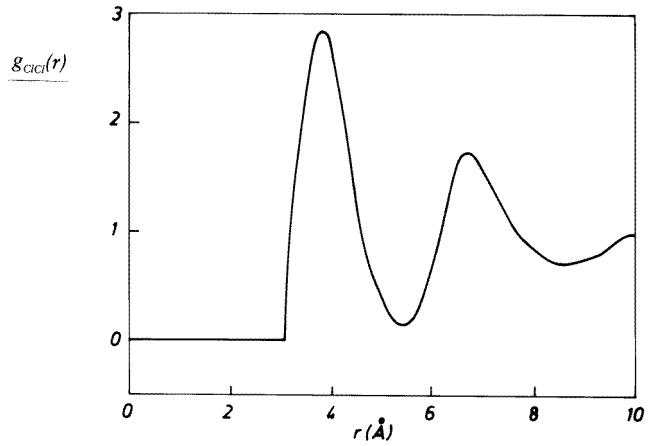

Figure 7. The radial pair distribution function $g_{ClCl}(r)$ for $LiCl \cdot 4D_2O$ glass at 120 K.

4. Discussion

4.1. Li^+ hydration structure

To understand the hydration structure of Li^+ in the glass, it is helpful to compare it with its structure in the liquid (figure 3). The main features of $G_{Li}(r)$ in the glass are the two peaks centred at 1.94 ± 0.03 and 2.53 ± 0.03 Å, which are identified with oxygen and deuterium atoms respectively. Integration under the first peak gives $\bar{n}^{O}_{Li} = 3.0 \pm 0.2$ atoms (table 3). From this result it is expected that the second peak will contain six deuterium atoms. However integration over the range $2.25 \leqslant r\,(\text{Å}) \leqslant 2.90$ shows that the peak can accommodate significantly more than this. In order to explain the additional amount, one concludes that other atoms must contribute to this peak. It is unlikely to be other hydrogen or oxygen atoms because of the high concentration of the solution (table 1). This is because 1.5 extra hydrogen or oxygen atoms would be required to be bound to the lithium ion and this would result in a hydration shell of 4.5 water molecules with very little ability of the water to share with other lithium ions. A more likely and preferred situation is one in which direct contact occurs between the positively charged Li^+ central ion and negatively charged near-neighbour Cl^- ions.

Similar results are obtained for the liquid [7], albeit with more water molecules in the first hydration shell and correspondingly less difference between the first and second peaks (table 3), a result which implies less encroachment by Cl^- in the liquid phase. A much larger difference was seen by Yamagami *et al* [18] whose results for $LiCl \cdot 5D_2O$ showed a decrease of coordination from four to three water molecules in the supercooled liquid phase between 213 and 173 K. They also report r_{LiO} and r_{LiD} distances of 2.02(5) and 2.61(5) Å respectively, which are significantly greater than the experimental results obtained here (table 3).

A second coordination shell is clearly evident, centred $\approx$4.3 Å. It is much more prominent than in the liquid (figure 3(*b*)) and signifies a sharpening of structure in the glass. This shell can accommodate seven chloride ions evenly distributed in the volume together with eight water molecules, whereas in the liquid this shell can only accommodate four chloride atoms and eight water molecules. This second coordination shell has also been

Table 3. The Li^+ hydration parameters derived from the present study and previous experimental studies of aqueous solutions of LiCl at ambient temperature unless stated otherwise.

Molality in D_2O	R (moles D_2O/salt)	r_{LiO} (Å)	r_{LiD} (Å)	$\bar{n}_{Li}^{D_2O}$	Reference
24.8 (130 °C)	2.02	1.95	2.31	2.3	[11]
16.66	3	2.5	2.71	4 ± 1	[10]
14.0	3.57	1.96	2.52	3.2 ± 0.21	[7]
12.5	4	2.22	2.68	4 ± 1	[10]
12.5 (120 K)	4	1.93	2.53	3.0 ± 0.2	this work
10	5	1.95	2.50	3.3 ± 0.5	[8]
6.25	8	1.95	2.43	4 ± 1	[10]
3.60	13.9	1.95	2.52	6.0 ± 0.4	[7]
3.57	14	1.95	2.55	5.5 ± 0.3	[8]
1.0	50.0	1.96	2.52	6.5 ± 1.0	[7]

identified by Yamagami *et al* (18) in the low temperature liquid, and was interpreted as an increase in the number of water molecules on cooling. However, we feel that the structural enhancement must be due to an increase in the number of Cl^- ions as this interpretation is more consistent with our results for $g_{ClCl}(r)$ (section 4.3).

4.2. Cl^- hydration structure

The total chloride ion radial distribution function, $G_{Cl}(r)$, for the aqueous lithium chloride glass (figure 5(*a*)) is similar in shape to that obtained in the liquid at 295 K (figure 5(*b*)), and to that in other electrolyte chloride solutions [5, 19]. However, for the glass, the first peak, at 2.23 Å, which is identified with nearest-neighbour hydrogen atoms, is much sharper than in the liquid and drops to a value close to $G_{Cl}(0)$ at $r = 2.8$ Å, suggesting a high degree of stability for this correlation. Integration over this peak gives a value for the Cl^- hydration of 4.8(3). As there are only four water molecules per lithium chloride unit, the Cl^- ions must share water molecules in the form of non-contact pairs bridged by water molecules. Evidence for bridged Cl^- pairs has already been demonstrated in the less concentrated aqueous solution of 8.6 molal lithium chloride [13], and in a more concentrated solution of 14.9 molal lithium chloride [6]. By simple interpolation of the data of the 14.9 and 9.98 molal solutions, one calculates that in the liquid $\bar{n}_{Cl}^{H} \cong 4.7$ atoms, a result in close agreement with the experimental data here (table 4).

The second feature of the $G_{Cl}(r)$ is centred at 3.3 Å and contains predominantly O and D atoms. In the glass, this compound peak has become partially resolved, with a first maximum at 3.29 ± 0.03 Å, which is identified with oxygen atoms from water molecules associated with the deuterium atom (D_1) at 2.23 Å. This implies stretching of O–D due to the strong polarizing effect of Cl^-. Recall in pure water O–D $\approx$ 0.98 Å with a half width of $\approx$0.5 Å. The low-r part of the peak at 3.29 Å was reflected about its maxima and integrated to give $\bar{n}_{Cl}^{O} = 5.5 \pm 0.5$, which is in reasonable agreement with that calculated for the first peak at 2.23 Å.

Generally one observes that $G_{Cl}^{glass}(r)$ has correlations to 12 Å, whereas the liquid $G_{Cl}(r)$ of both 14 molal [16] and 9.98 molal solutions [15] terminates at $\sim$4.0 Å. The additional structure in the glass must be related to indirect correlations between chloride ions. In total three hydration shells out to 12 Å can be identified; these are smeared out in the liquid, presumably because the water molecules are in fast exchange around the Cl^-.

Table 4. The Cl^- hydration parameters derived from the present study and previous experimental studies of aqueous solutions of LiCl at ambient temperature unless stated otherwise.

Molality in D_2O	R (moles D_2O/salt)	r_{ClD_1} (Å)	r_{ClO} (Å)	r_{ClD_2} (Å)	$\bar{n}_{Cl}^{D_2O}$	Reference
14.9	3.35	2.24	3.25	3.56	4.4 ± 0.3	[6]
14.0	3.57	2.24	3.27	3.54	4.4 ± 0.3	[9]
12.5 (120 K)	4	2.23	3.29	3.50	4.8 ± 0.3	this work
9.98	5	2.22	3.29	3.50–3.68	5.3 ± 0.2	[19]
8.3	6	2.225	3.2	3.625	5.4	[12]
8.3 (125 K)	6	2.225	3.175	3.625	5.4	[12]
3.57	14	2.25	3.34	—	5.9 ± 0.2	[19]

Table 5. The properties of the $g_{ClCl}(r)$ measured in different lithium chloride solutions: r_1, r_{M_1} and r_{M_2} are respectively the cut-off distance and the positions of the first and second maxima.

	r_1 (Å)	r_{M_1} (Å)	$\bar{n}_{Cl}^{Cl}$	r_{M_2} (Å)	$\bar{n}_{Cl}^{Cl}$	Reference
12.5 molal 120 K	3.1	3.90	3.6 ± 0.5	6.4	8.5 ± 1.5	this work
14.9 molal 293 K	3.0	3.75	2.3 ± 0.3	6.38	10.0 ± 1.5	[9]
8.6 molal 295 K	3.9	4.2	1.2 ± 0.5	6.4	7.0 ± 0.5	[13]

4.3. The ion–ion structure

Although a determination was made of $g_{LiLi}(r)$ from the three functions ${}^{6}_{NAT}F(Q)$, ${}^{\phi}_{NAT}F(Q)$ and ${}^{7}_{NAT}F(Q)$, it was found that the resulting function was unphysically large and no useful information could be extracted.

The pair correlation function $g_{ClCl}(r)$ (figure 7) derived from Fourier transformation of $S_{ClCl}(Q)$ (13) shows two prominent peaks at 3.9 ± 0.2 and 6.4 ± 0.2 Å with coordination numbers, $\bar{n}_{Cl}^{Cl}$, of 3.6 ± 0.5 and 8.5 ± 1.5 respectively. The discussion of $g_{ClCl}(r)$ is best conducted in comparison with $g_{ClCl}(r)$ for the two liquids: 14.9 molal $LiCl_{(aq)}$ [6], and 8.6 molal $LiCl_{(aq)}$ [15]. The main characteristics of $g_{ClCl}(r)$ in these three systems are listed in table 5. The first peak at 3.90 Å in the glass is almost exactly at the same position as that calculated from a linear interpolation from the peak positions of 14.9 molal and 8.6 molal solutions. However, the coordination number is twice that for the liquid at a similar concentration. This can be explained by considering the water molecules, anions and cations together. In the glass, the effective free volume of the Cl^- coordination shell will be larger due to a reduction in thermal vibration of the water molecules, which will facilitate direct $Cl^- \ldots Cl^-$ contacts without a reduction in hydration number. In contrast, the smaller Li^+ with its relatively stronger electrostatic interaction will not benefit in free volume to the same extent. However, the reduction in $\bar{n}_{Li}^{O}$ from $\sim$4 to $\sim$3 suggests that $Li^+ \ldots Cl^-$ contacts can occur. The picture overall therefore is one in which the direct $Cl^- \ldots Cl^-$ contacts are stabilized by the Li^+ hydration shell and a water bridge. The implication for this model is that in cases where the cation is not strongly hydrated, e.g. K^+, Sr^{2+}, no additional direct contacts will take place when a system is glassified. Conversely in the case of even stronger cation hydration, e.g. Ni^{2+}, Fe^{3+}, ..., we would predict that in the glass there will be an increased probability of direct $Cl^- \ldots Cl^-$ contacts over that in the liquid.

The second peak in the $g_{ClCl}(r)$ is at a similar distance to Cl^-–Cl^- distances seen at the 14.9 molal and 8.6 molal LiCl solution and is interpreted as indirect chloride pairs which

are bridged by a water cation complex. In the glass, the coordination number of 8.5 is, as might be expected, intermediate between the values of ten and seven in the two liquids (table 5).

5. Conclusions

The most important observation from the above study is that, compared to the liquid, the glass has a higher number of ion pairs and ion clusters, which force the water molecules into an 'edge-on' position in the cluster. The readiness of glass formation is conditioned by the ability of the water molecules abetted by the strongly hydrated Li^+ ion to produce relatively stable clusters of ions and water molecules. Good glass forming concentrations of aqueous lithium chloride are, therefore, those in which there is a sufficient number of water molecules to fill the first hydration spheres of the ions but not enough to allow an extended hydrogen bond network to be formed between the ion clusters. This hypothesis could explain the complicated glass phase diagram of $LiCl \cdot nH_2O$ and could be investigated experimentally by a study of the hydrogen bond network, in the crystalline, liquid and glass states, at different concentrations.

Acknowledgments

The authors wish to thank Dr Marie-Claire Bellissent-Funel and M Jean-Pierre Ambrose (CEN Saclay, France) for their help with the neutron diffraction experiments and Dr Ian Howell for access to unpublished results. We also thank EPSRC for financial support.

References

[1] Angell C A and Sare E J 1970 *J. Chem. Phys.* **52** 1058
[2] Dupuy J, Elarby-Aouizerat A, Claudy P, Jal J-F, Letoffe J M and Chieux P 1987 *Aqueous Ionic Solutions* NATO ASI C205, ed M-C Bellissent-Funel and G W Nielson (Dordrecht: Reisel) p 447
[3] Preval B, Jal J-F, Dupuy-Philon J and Soper A K 1995 *J. Chem. Phys.* **103** 1897
[4] Preval B, Jal J-F, Dupuy-Philon J and Soper A K 1995 *J. Chem. Phys.* **103** 1886
[5] Neilson G W and Enderby J E 1996 *J. Phys.: Condens. Matter* **100** 1317
[6] Copestake A P, Nielson G W and Enderby J E 1985 *J. Phys. C: Solid State Phys.* **18** 4211
[7] Howell I and Neilson G W 1996 *J. Phys.: Condens. Matter* **8** 4455
[8] Newsome J R, Neilson G W and Enderby J E 1980 *J. Phys. C: Solid State Phys.* **13** L923
[9] Howell I 1993 *PhD Thesis* University of Bristol
[10] Narten A H, Vaslow F and Levy H A 1973 *J. Chem. Phys.* **58** 5017
[11] Ichikawa K, Kameda Y, Matsumoto T and Misawa M 1984 *J. Phys. C: Solid State Phys.* **17** L725
[12] Jal J-F, Soper A K, Carmona P and Dupuy J 1991 *J. Phys.: Condens. Matter* **3** 551
[13] Ansell S 1995 *PhD Thesis* University of Bristol
Ansell S and Neilson G W in preparation
[14] Vogel I 1953 *Macro and Semimicro Qualitative Inorganic Analysis* (London: Longmans)
[15] BDH 1980 *Ion Exchange Methods* (Poole, UK: BDH)
[16] Powell D H, Neilson G W and Enderby J E 1989 *J. Phys.: Condens. Matter* **1** 8721
[17] Soper A K 1989 *Inst. Phys. Proc. 97* (Bristol: Institute of Physics) p 711
[18] Yamagami M, Yamaguchi T, Wakita H and Misawa M 1994 *J. Chem. Phys.* **100** 3122
[19] Cummings S, Enderby J E, Neilson G W, Newsome J R, Howe R A, Howells W S and Soper A K 1980 *Nature* **287** 5784